A Simple and Highly Stable Porous Gold-based Electrochemical Sensor for Bisphenol A Detection

Rodtichoti Wannapob,[a, b, c] Panote Thavarungkul,[a, b, d] Supaporn Dawan,[a, b, c] Apon Numnuam,[a, b, c] Warakorn Limbut,[a, b, e] and Proespichaya Kanatharana*[a, b, c]

Abstract: A porous gold electrode with a uniform pore size was prepared by a simple single potential step method. It provided around 19 times more surface area than a bare gold electrode. The porous gold electrode, without any modification, exhibited good electrocatalytic activity towards the oxidation of bisphenol A (BPA). The effect of the pH and scan rate, on the porous gold electrode was studied and discussed. Under optimum conditions of the flow system, the calibration plot of BPA was linear over a wide range of concentration, from 2.0 nM to 800 nM ($R^2 = 0.999$), and the detection limit was 2.0 nM (s/n = 3). It was of interest that, the porous gold electrode showed an exceptional result in minimizing the fouling from the oxidation product of BPA and led to a very high operational stability of the electrode for the detection of BPA (560 consecutive times). The porous gold electrode showed good fabrication reproducibility and can be used to detect bisphenol A that leached from baby bottles and drinking water bottles. The obtained results were in good agreement with the GC-MS method ($P > 0.05$).

Keywords: Porous Gold · Bisphenol A Detection · Reduce fouling effect · Electrochemical Sensor

1 Introduction

Bisphenol A (BPA) is a monomer and plasticizer used in the production of polycarbonate plastic [1] that is widely used in many consumer products such as baby bottles and beverage containers [2]. The leaching of BPA from these containers can lead to human exposure [1], and it is especially important from products for young children [3]. BPA is identified as an endocrine disrupting compound. It can mimic and interfere with hormonal activities by disrupting growth, development and reproduction. It is also a possible cause of reproductive cancers such as testicular, prostate, breast, uterine and ovarian [1]. As a result, many polycarbonate plastic based products have now been modified to replace BPA with new copolymers such as co-polyesters [4]. However, a recent study by the Joint Research Centre, European Commission [5] indicated that possible problems derived from the use of these alternative plastics have not yet been thoroughly evaluated [4,6]. Therefore, the use of BPA is still quite common and human exposure to BPA should still be monitored [7]. In such case a fast, simple and accurate method for BPA detection would be potentially useful and an electrochemical method would be extremely attractive due to its fast response, it is a relatively cheap instrument, simple to use, it can have a high sensitivity and is useful for real-time detection.

It is possible to electrochemically detect BPA because its phenolic hydroxyl groups can be oxidized at an electrode surface. However, oxidation on a bare electrode surface needs a high overpotential and the sensitivity is poor [8]. This restriction can be overcome by modifying the electrode with some materials, i.e., thionene [9], cobalt phathalocyanine [10], mesoporous silica [11], Mg-Al-CO$_3$ layered double hydroxide [12], polyglutamic acid (PGA)/amino-functionalised carbon nanotubes [13], polyaniline nanorods and multi-walled carbon nanotube [14] and Poly(3,4-ethylenedioxythiophene)(PEDOT) [15]. However, these modified electrode surfaces are still gradually passivated due to the formation of a polymer product during the oxidation process, which decreases the sen-

[a] R. Wannapob, P. Thavarungkul, S. Dawan, A. Numnuam, W. Limbut, P. Kanatharana
Trace Analysis and Biosensor Research Center
Prince of Songkla University
Hat Yai, Songkhla 90112, Thailand

[b] R. Wannapob, P. Thavarungkul, S. Dawan, A. Numnuam, W. Limbut, P. Kanatharana
Center of Excellence for Innovation in Chemistry, Faculty of Science
Prince of Songkla University
Hat Yai, Songkhla 90112, Thailand

[c] R. Wannapob, S. Dawan, A. Numnuam, P. Kanatharana
Department of Chemistry, Faculty of Science
Prince of Songkla University
Hat Yai, Songkhla 90112, Thailand
Tel: +66-74-288420, Fax: +66-74-558841
*e-mail: proespichaya.k@psu.ac.th

[d] P. Thavarungkul
Department of Physics, Faculty of Science
Prince of Songkla University
Hat Yai, Songkhla 90112, Thailand

[e] W. Limbut
Department of Applied Science, Faculty of Science
Prince of Songkla University
Hat Yai, Songkhla 90112, Thailand

sitivity and the life time of the electrode [13,15]. To regenerate the surface, a cycling potential can be applied after each electrochemical measurement to remove the unwanted material [13]. However, this additional step increases the analysis time. So, the development of an electrochemical sensor with better properties such as ease of manufacturing, low cost and with a minimal or no fouling effect is still a challenge.

An interesting approach was to make use of the excellent electrocatalysis properties of a nanostructured transition metal such as Au [16], Ni [17] and Pt [18]. Among these, gold is the most studied due to its chemical stability and unique surface chemistry. For detection of BPA, gold nanoparticles have been used to fabricate chemical sensors together with a poly(amidoamine) [19], molecular imprinted polymer sol-gel [20], and carbon nanotubes [21]. However, gold nanoparticles have a strong tendency to agglomerate, which reduces the active surface area [22]. As an alternative, porous gold, a new kind of material can circumvent this problem. Its high porosity, hence, formation a large surface area to volume ratio will also provide excellent performances and good electrocatalytic properties.

Porous gold films have been used for the electrochemical detection of a number of compounds such as glucose [22], human serum chorionic gonadotropin [23] and kanamycin [24]. A common fabrication process to produce a porous gold film is by the alloying and dealloying method, which is simple and reproducible method. However, it requires a number of steps to fabricate the porous structure. An interesting alternative method has been reported by Deng and coworker [25]. This one-step electrochemical strategy can fabricate a porous gold film electrode by applying a potential step to a bare gold electrode in HCl solution. Compared with the dealloying strategy, this method is easier and more rapid.

In this work, a porous gold electrode, fabricated by a one-step electrochemical method, was investigated as an alternative surface to lessen the fouling effect on the electrode surface for BPA detection. Details study of the BPA oxidation at the porous gold surface with an emphasis on its potential application as an unmodified electrode are presented. The large surface area of the porous gold together with its high electrocatalytic property were used to enhance the response of BPA leached from baby and drinking water bottles into water and to minimize the effect of fouling of the electrode surface that helped to increases the life time of the electrode.

2 Experimental

2.1 Reagents and Apparatus

Bisphenol A, phenol, p-nitrophenol, 2,4-dinitrophenol and 2,4-dicholophenol were from Sigma-Aldrich Chemical Co. (St. Louis, Mo, USA). A BPA stock solution of 0.10 M, was prepared with acetonitrile (Lab-Scan, Bangkok, Thailand) and kept at 4 °C. Phosphate buffer solu-

tions (0.1 M) with various pH values were prepared with Na_2HPO_4 and NaH_2PO_4 and adjusted by 0.1 M H_3PO_4 or 0.1 M NaOH solutions. All other reagents were of analytical reagent grade and used as received without further purification. All solutions were prepared with deionized water that was treated by a reverse osmosis system and purified with a Maxima ultrapure water instrument (ELGA, England) to obtain a resistivity of 18.2 MΩ.cm. Electrochemical experiments were performed with a μ-Autolab type III (Metrohm Autolab, B.V., The Netherlands). A three electrode system was used with a gold rod working electrode (3.0 mm in diameter, surface area 0.0707 cm^2, purity ≥ 99.99%), a platinum wire counter electrode and a Ag/AgCl (3.0 M KCl) reference electrode. The gold electrode surface morphology was investigated by a JSM-5200 Scanning electron microscope (SEM) (JEOL, Japan).

A flow injection system was employed for the analysis of BPA. The detection chamber was a flow cell with three electrodes, i.e., a porous gold working electrode, a platinum wire auxiliary electrode, and a custom-made Ag/AgCl reference electrode. A peristaltic pump (Miniplus 3, Gilson, France) was used to deliver the carrier solution while a six-port valve (Valco, Houston, TX, USA) was used as the sample injector to control the exact sample volume.

2.2 Fabrication of the Porous Gold Electrode

A gold rod electrode was first mechanically polished with alumina slurries (particle size 5.0, 1.0 and 0.3 μm), cleaned in 0.50 M H_2SO_4 by cyclic voltammetry between 0.10 and 1.50 V at a scan rate of 0.10 V s^{-1} for 25 scans and dried with a stream of nitrogen gas. The method to fabricate the porous gold electrode was as described by Deng and co-worker [25]. In brief, the three electrodes, a platinum wire counter electrode, Ag/AgCl reference electrode and the cleaned gold working electrode were immersed in 5.0 mL of 2.0 M HCl in a 10 mL beaker. The surface of gold electrode was parallel to the bottom of the beaker (Figure 1). A step potential was applied from the open circuit to 1.50 V for 100 s. This potential is the initial transition region of gold [25]. The 100 s was chosen from a preliminary study to be the length of time that enabled the entire electrode surface to be covered by the porous structure.

2.3 Characterization of Porous Gold Films

The morphology of the fabricated porous gold electrodes was observed by scanning electron microscopy (SEM) (JEOL JSM-5200). The total active area of the porous surface was investigated by cyclic voltammetry in 0.50 M H_2SO_4 via the roughness factor of the electrode estimated from the charges to form the gold oxide monolayer on the gold surface based on the oxygen adsorption measurement [26]. The thickness of the porous layer was

measured from an SEM image of the side view of the electrode by a digital caliper (Kovet, Taiwan).

2.4 Optimization of the Flow System

The effect of several parameters on the amperometric response of BPA in this flow injection system was investigated by the univariate method (changing one parameter and keeping others constant) in order to achieve a compromise between a high response and short analysis time. These included the effect of the applied potential, pH and concentration of the carrier buffer, flow rate and sample volume.

2.5 Baby and Drinking Water Bottles Sample Preparation

Six brands of baby bottles and three brands of drinking water bottles, which were made from polycarbonate plastic were purchased from local super-markets and flea market. The leaching was tested by adding 100 mL of 40 °C and 100 °C water into the baby bottles and 40 °C water into the drinking water bottles, then shaking for 1 h (wrist action shaker, model 75, Burrell corporation, USA). These water samples were divided into two portions. One was analysed by the proposed method and the other by the GC-MS method (Agilent, USA). For the analysis with GC-MS, the BPA was extracted from 5.0 mL of each sample by adding 5.0 mL of ethyl acetate (EtOAc) and by sonication for 1 h.

3 Results and Discussion

3.1 Fabrication and Surface Characterization of the Porous Gold Electrode

The porous gold was fabricated by applying a potential at the transition region of gold in HCl solution. The mechanism includes electrodissolution, disproportion and deposition as described previously by Deng and co-workers [25]. The key point of the method is the potential at the transition of gold. At this potential, gold was dissolved by the electrodissolution process under the limiting diffusion of Cl^- and forming complex with Cl^-. This was followed by the disproportionation of $AuCl_2^-$ into gold atoms and $AuCl_4^-$ due to the depletion of Cl^- near the surface. Finally the gold atoms aggregated and deposited on the rough surface of electrode to form porous structure [25]. The distance between the surface of the gold electrode and the beaker bottom also affected the fabrication of the porous gold. If the gap was too large (Figure 1A), the soluble complex would diffuse away from the electrode surface, so the porous gold could not be produced. In this work a suitable distance was found to be at 1.5 mm (Figure 1B), with this distance the porous gold structure is completely formed on the surface of electrode. Figures 2A and 2B show the SEM images of a bare and a porous gold surface. The pore formation and the coverage on the gold surface were extremely uniform when ob-
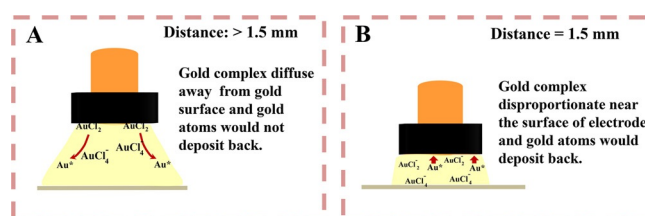

Fig. 1. The formation of porous structure on gold surface (A) no deposition of gold when the distance between the electrode surface and the beaker bottom was more than 1.5 mm, (B) gold deposition at distance between the electrode surface and beaker at 1.5 mm.

served at a lower magnification (Figure 2C). The thickness of the porous layer was measured at 150 different positions from the side view of the 3.0 mm diameter porous gold electrode SEM image. The porous layer had a shape of a flat dome with a thickness of 0.012 mm at the edge up to 0.148 mm in the center. The average thickness is 0.11 ± 0.04 mm.
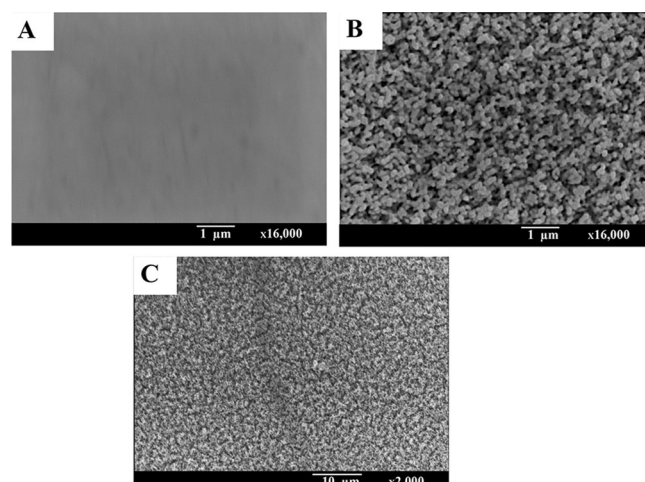

Fig. 2. SEM images of (A) bare gold electrode (B) and (C) porous electrode with different enlargement scales.

To express the ratio between the real surface area and the geometrical area of the electrode, the charge associated with the reduction of the gold oxide that was proportional to the real active surface area of the gold electrode [26] was determined by cyclic voltammetry.

The cyclic voltammogram of the porous gold electrode (Figure 3a) showed a clear increase of the cathodic peak at +0.90 V compared to the bare surface electrode (Figure 3b). The roughness factor of the electrode was calculated by integrating the reduction of the charge of the gold oxide peak in the cyclic voltammogram (the shaded area in Figure 3a) then divided by 400 µC/cm^2 [26]. This value of the porous gold surface was 19 ± 1 times (20 electrodes) that of the bare gold electrode of the same diameter.

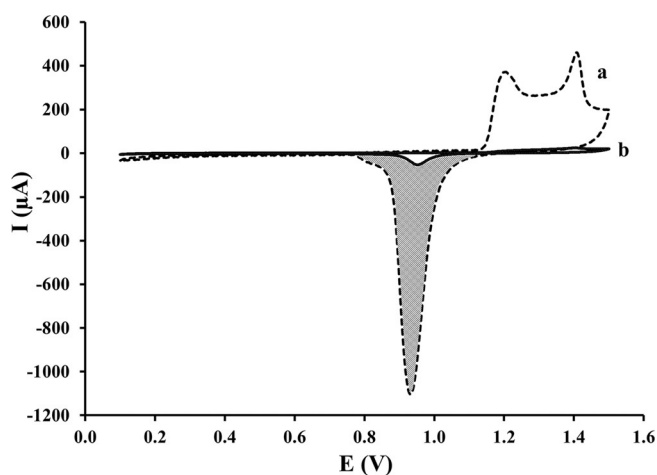Fig. 3. Cyclic voltammograms of gold substrates obtained at $100 \, mV \, s^{-1}$ in 0.50 M H_2SO_4 (a) a porous gold electrode (dashed line), (b) a bare gold electrode (solid line).

3.2 Electrooxidation of BPA

Cyclic voltammograms of the oxidation of 0.25 mM BPA in 0.10 M phosphate buffer pH 6.00 containing 0.10 M KCl with a bare and a porous gold electrodes are shown in Figure 4A. At the surface of the bare gold electrode (Figure 4A (a)), the oxidation peak of BPA appeared at +0.70 V. This was slightly shifted to a more negative value (+0.65 V) for the porous gold electrode (Figure 4A (b)). Furthermore, the background current of the porous electrode (3.5 µA) was more than that of the bare gold electrode (0.86 µA) and its oxidation peak current with BPA was much higher, i.e., 8.83 µA compared to 3.57 µA. This behavior is most likely due to the large surface area of a three dimensional gold porous network and its fast electron transfer capability. In the reverse scan there was no observable peak for either electrodes and this indicated that the oxidation of BPA on the gold electrode was a totally irreversible reaction [14,19,21].

The increment of oxidation peak current for BPA at porous gold (2.47 times) was not as much as that expected based on the increment of the surface area (19 ± 1 times). This is probably due to the fast electron transfer of BPA [27], hence, the BPA can be completely oxidized on the top part of the porous structure before it can diffuse down further into the porous system. This is in contrast to a remarkable increase in electrochemical signal when the porous gold electrode was employed with a slow electron-transfer kinetics chemical [28]. Thus, in this work the inner porous surface may not play a significant role in the performance of the electrode at the beginning, but this extra surface would be very useful in lessening the fouling affect. It is generally known that a major problem related to the oxidation of phenolic compounds on a bare electrode was the production of a polymer of the product on the electrode surface as shown in previous work [29], thus, reducing its active sur-
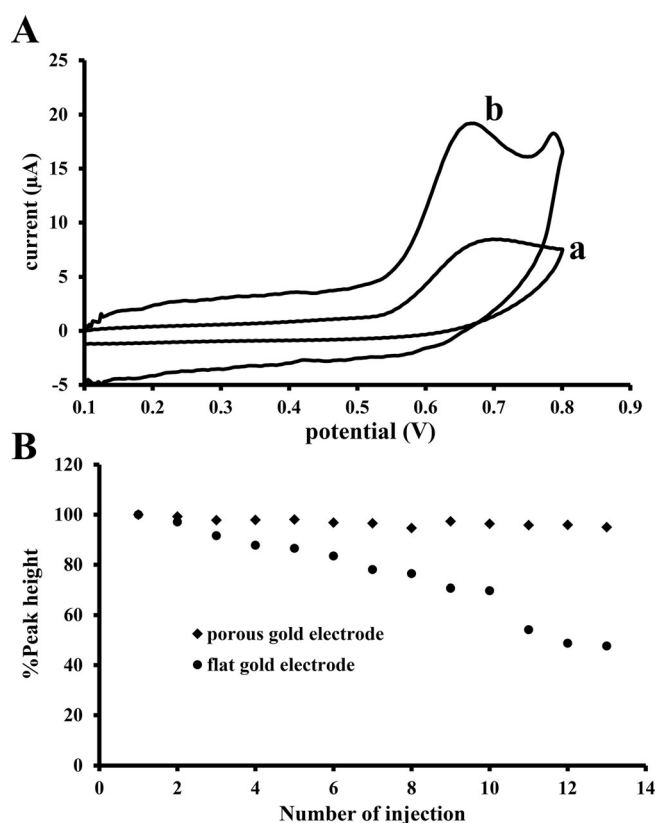

Fig. 4. (A) Cyclic voltammograms of (a) bare gold electrode (b) porous gold electrode in 0.25 mM BPA in 0.10 M phosphate buffer solution (pH 6.00) containing 0.10 M KCl at scan rate: $100 \, mV \, s^{-1}$, (B) Relative peak height of a porous gold and a bare gold electrode from repeated injection of 0.25 mM BPA in a flow system.

face area. Figure 4B shows a comparison of the oxidation currents with 0.25 mM BPA. For a bare gold electrode the oxidation current decreased immediately after the first injection and to about 50% after 12 injections. In contrast, the fouling on the large surface area of the porous gold electrode has less effect and the relative response after thirteen injections only decreased by 5.0%.

To confirm the existence of a polymeric film produced on the electrode surface during the oxidation of BPA, infrared spectroscopy (FTIR-ATR) was used to characterize the electrode surface before and after BPA oxidation (Supporting Information Figure S1). The IR spectrum after BPA oxidation exhibited some bands that could not be observed on the gold surface before BPA oxidation. These include two bands at $2929 \, cm^{-1}$ and $2862 \, cm^{-1}$ due to the C–H stretching. The bands in the $1630–1700 \, cm^{-1}$ region can be associated with the C=O stretching. Another two bands at $1461 \, cm^{-1}$ and $1513 \, cm^{-1}$ referred to the symmetrical stretching of C=C. This spectrum is similar to the one obtained in a previous work in which a film obtained during oxidation of BPA was studied [30]. These results indicated that a polymeric BPA film was formed on the gold electrode surface.

3.3 Effect of pH

The pH of a supporting electrolyte will generally influence the oxidation reaction process [31]. The oxidation of BPA on the porous gold electrode was investigated between pH 5.00 and 10.00 (0.10 M phosphate buffer) by cyclic voltammetry. The highest peak current was produced at pH 6.00 (Supporting Information Figure S2A) which was lower than the pK$_a$ of BPA (pK$_a$=9.73) [32]. This, indicated that the non-dissociated BPA was adsorbed onto the porous gold surface better than the dissociated BPA [33]. A 0.10 M pH 6.00 phosphate buffer containing KCl 0.10 M was then chosen as a supporting electrolyte for subsequent experiments. In addition, a negatively shifting oxidation peak potential of BPA was also observed with an increasing pH, and this indicate that protons had been involved in the oxidation process. A plot of E_{pa} versus pH (Supporting Information Figure S2B) showed a linear relationship with a slope of −0.0589 V/pH. This is almost the same as the theoretical value of −0.059 V/pH to indicate that an equal number of protons and electrons were involved in the BPA oxidation process [34].

3.4 Effect of Scan Rate

To obtain more information on the kinetic and transport processes of the oxidation of BPA on the porous gold electrode, the effect of the cyclic voltammetry scan rate (ν) was investigated with the supporting electrolyte. The cyclic voltammograms of 0.10 mM BPA showed that the oxidation peak current increased with the scan rate (Supporting Information Figure S3 inset). A linear relationship between the oxidation peak current and the square root of the scan rate was obtained between 20 and 500 mV s^{-1} (Supporting Information Figure S3) and this indicated that within these scan rates the range of the kinetics of the overall process of BPA oxidation at the porous gold electrode was controlled by a diffusion process [35]. In addition, the oxidation peak potential shifted positively with an increase of the scan rate. The variation of the peak potential (E_{pa}) with a scan rate (ν) of between 20 and 500 mV s^{-1} followed the linear regression equation: E_{pa} (V)=0.54+0.056 log ν, R^2=0.997. For a totally irreversible anodic reaction, the linear relationship between E_{pa} and ν could be written as:

$$E_{pa} = A + \frac{2.3RT}{(1-\alpha)nF} \log \nu \qquad (1)$$

Where A is a constant related to the formal electrode potential (E°) and the standard rate constant at E°; n is the number of the electrons transferred; F is the Faraday constant (96,500 C mol^{-1}); α is the charge transfer coefficient, R and T have their usual meaning. Generally, α is assumed to be 0.5 in the totally irreversible electrode process [36]. From Eq. 1 and the slope of E_{pa} versus logν, the electron number (n) can be calculated to be 2. From the results obtained in the pH investigation (3.3), an equal number of electrons and protons were involved in the oxidation process of BPA, therefore, the electrochemical oxidation of BPA on a gold porous electrode was a two-proton and a two-electron transfer process. This is consistent with earlier reports [12,19,21,33–34,37]. Thus the possible reaction pathways for BPA oxidation on the porous gold electrode is proposed to be as shown in Scheme 1, which is in good agreement with previous reports [37].

3.5 Flow Injection Analysis of BPA

The effect of several parameters on the amperometric response of BPA oxidation in a flow system (Supporting Information Figure S4) using the porous gold electrode was studied by injecting a series of different concentration of BPA (100, 200, 300, 400 and 500 nM). The detection chamber of the flow cell (10 μL) was in contact with a porous gold working electrode, a custom-built Ag/AgCl reference electrode and a platinum wire counter electrode.

3.5.1 Hydrodynamic Voltammetry

From the potential range of the BPA oxidation peak in the cyclic voltammogram, the appropriate potential for the detection of BPA was tested at +0.55, +0.60, +0.65, +0.70 and +0.75 V. The best sensitivity (slope of the calibration plot) was obtained at +0.65 V (0.156± 0.003 nA nM^{-1}). It is most likely that at this potential the oxidation of BPA occurred on the active gold surface without the formation of gold oxide [35], thus showing the highest sensitivity. When the potential was higher than +0.65 V, the gold oxide might form on the surface and inhibit the oxidation of BPA [38]. On the other hand, at a value lower than +0.65 V the potential had not reached the oxidation peak, hence, the BPA was only partially oxidized. Thus, a working potential at +0.65 V was chosen for the amperometric measurements in the flow system. This is the same potential at which the maximum current was observed when the voltammetric curves were recorded in static conditions (Figure 4A).

3.5.2 Sample Volume

The analytical signal was also dependent on the sample volume and its effect on the sensitivity of the porous electrode was investigated at 200, 250, 300, 350, and 400 μL. The sensitivity was 0.1454±0.0028 nA nM^{-1} for 200 μL, and increased with the sample volume and became steady from 350 μL onwards (0.1893±0.0031 nA nM^{-1}). Therefore, 350 μL was chosen because it provided the highest sensitivity with the shortest analysis time.
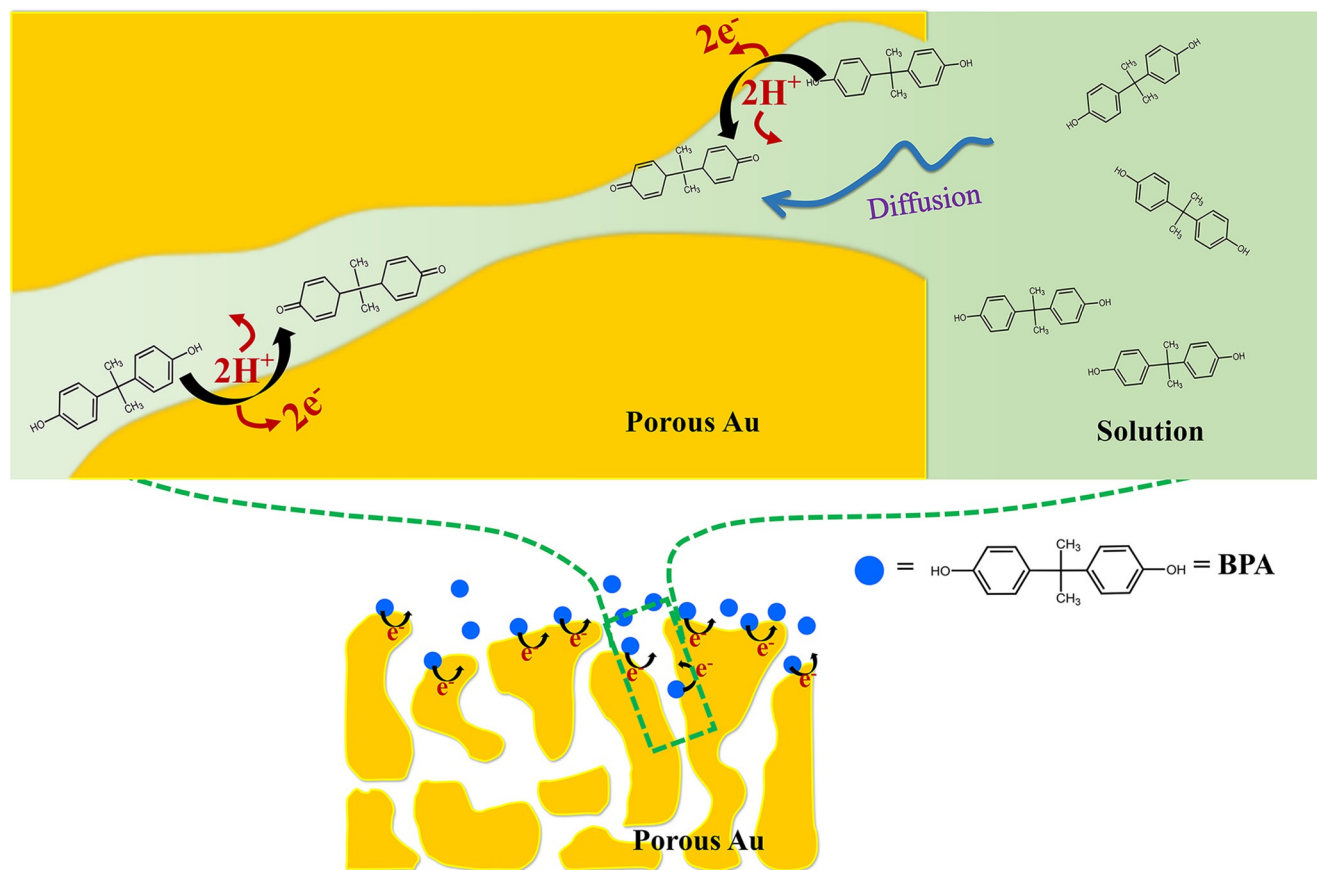
Scheme 1. Proposed reaction mechanism for the oxidation of bisphenol A on porous gold electrode.

3.5.3 Flow Rate

The flow rate of the carrier buffer was investigated at 200, 300, 400, 500, 600, 700, 800 and 900 $\mu L\,min^{-1}$. An increase in the flow rates usually leads to a change in the diffusion profile at the electrode surface and increases the efficiency of the mass transport. The sensitivity of the response increased with the flow rate from 0.1570 ± 0.0050 $nA\,nM^{-1}$ at 200 $\mu L\,min^{-1}$ up to 0.1970 ± 0.0039 $nA\,nM^{-1}$ for 800 $\mu L\,min^{-1}$ and then decreased. The increase of sensitivity from 200 to 800 $\mu L\,min^{-1}$ was due to the increase of the mass transfer of BPA to the electrode surface and the reduction of the dilution of the sample concentration, so a sharper and higher peak current was obtained with an increase of the flow rate. The decrease of the sensitivity at 900 $\mu L\,min^{-1}$ was due to the low sample residence time in the reaction flow cell. Thus, a flow rate of 800 $\mu L\,min^{-1}$ was selected for subsequent studies.

In summary, the optimum conditions were: an applied potential of $+0.65$ V; a carrier buffer of 100 mM of sodium phosphate at pH 6.00; a flow rate of 800 $\mu L\,min^{-1}$ and a sample volume of 350 μL. These conditions were used for all remaining experiments which provided an analysis time of about 3 min.

3.6 Performance of the Modified Electrode

3.6.1 The Linear Dynamic Range and Detection Limit

The responses of the porous gold electrode to various concentrations of BPA are shown in Figure 5. A linear relationship was obtained between 2.0 and 800 nM and the detection limit was 2.00 ± 0.24 nM (S/N=3). Table 1
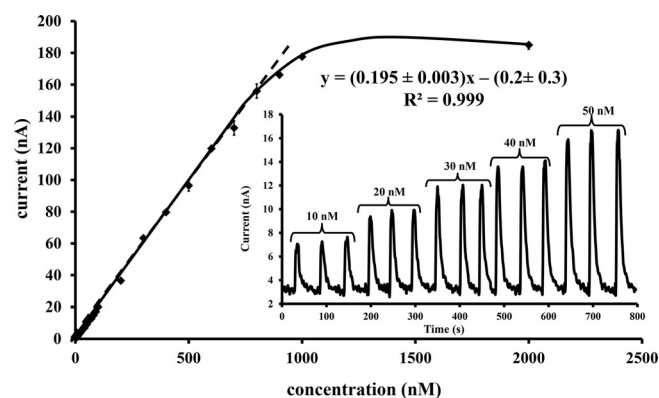

Fig. 5. The calibration curve of BPA from 2.0–2000 nM (n=3) and example of the current response of BPA concentrations from 10 nM to 50 nM in the flow injection analysis (inset).

Table 1. Comparison of the porous gold electrode performance with other modified electrodes using electrochemical detection of BPA.

Sensors	Linear range	Detection Limit	Reference
PEDOT-GCE	40–410 μM	22.0 μM	[15]
TPGE-LP/SH	0.05–5.0 μM	3.1 nM	[44]
PANI nanorods/MWNTs/PEG	1.0–400 μM	10.0 nM	[14]
AuNPs/MoS$_2$/GCE	0.05–100 μM	5.0 nM	[39]
PAMAM–Fe$_3$O$_4$/GCE	0.01–3.07 μM	5.0 nM	[33]
C60/GCE	74–230 nM	3.7 nM	[8]
Bi$_2$WO$_6$–CPE	50–2300 nM	20.0 nM	[45]
Aptamer/Nanoporous gold	0.1–100 nM	0.056 nM	[41]
Peptide/Au	1–5000 nM	0.7 nM	[42]
SWCNTs/Nanoporous gold	0–5 μM	100 nM	[46]
Nanoporous gold/GCE	0.1–50 μM	12.1 nM	[40]
Porous gold electrode	2.0–800 nM	2.0 nM	This work

shows the comparison of the performance of electrochemical sensors with different modified electrodes reported for BPA detection. This work provided the widest linear range and also lower detection limit compared to other composite i.e. PEDOT [15], C60 [8], PAMAM-Fe$_3$O$_4$ [33], AuNPs/MoS$_2$ [39] modified GCE. Comparing this porous gold electrode to other nanoporous gold electrodes for BPA detection, this porous gold electrode with a flow system exhibited a wider linear range and lower detection limit than the nanoporous gold modified GCE [40]. However, this detection limit was not as good as those of the electrochemical biosensors for BPA in which the nanoporous gold electrode and gold electrode were modified by aptamer [41] and peptide [42]. Although, the detection limit is not as low as those of the biosensors, it is sufficient to determine the BPA safety value (22 nM [3]). The wide linear range and the low detection limit could be attributed to the large surface area of the porous gold and this will be very useful for the detection of low levels of BPA in real samples.

3.6.2 Interference Effect

To evaluate the selectivity of the sensor, the influence of some phenolic compounds and inorganic ions were examined separately and compared to signal of 50 nM BPA. The results showed that a 100-fold concentration of 2,4-dicholophenol, 2,4-dinitrophenol and phenol had no influence on the signal of BPA with maximum deviations of below 10 % (Supporting Information Table S1). In addition, some inorganic ions that may exist in water such as a 500-fold concentration of Na^+, Ca^{2+}, Mg^{2+}, Fe^{3+}, Ni^{3+}, Cl^-, SO_4^{2-}, NO^{3-}, also had no influence on the signal of BPA.

3.6.3 Operational Stability

The operational stability of the porous gold electrode was investigated in a continuous operation mode by repeatedly injecting 100 nM of BPA in carrier buffer. The oxidation of BPA was maintained at no less than 90 % of the initial values for 560 injections (Figure 6). The first 548

injections yielded a 98 ± 3 % of its original response (relative standard deviation = 3 %). This good long-term stability of the porous electrode was attributed to the ability of the large surface area of the porous structure to lessen the effect of surface fouling. It is likely that when the outer part of the porous electrode, which is located closest to the electrolyte, initially reacted with the BPA and become non-reactive due to fouling, the BPA in the sample carried by the flow could reach the porous part of the electrode beyond the fouled part of the film so was still detected and this also increased the electrode life [43].

3.6.4 Repeatability

To investigate the repeatability of the porous gold preparation method, seven porous electrodes fabricated on the same day were used to examine BPA at five different concentrations selected from the linear range (100 nM, 200 nM, 300 nM, 400 nM and 500 nM). The relative standard deviations (RSDs) of the current responses of every concentration were all very low, maximum at 3.3 % (Supporting Information Figure S5A), and the RSD of the
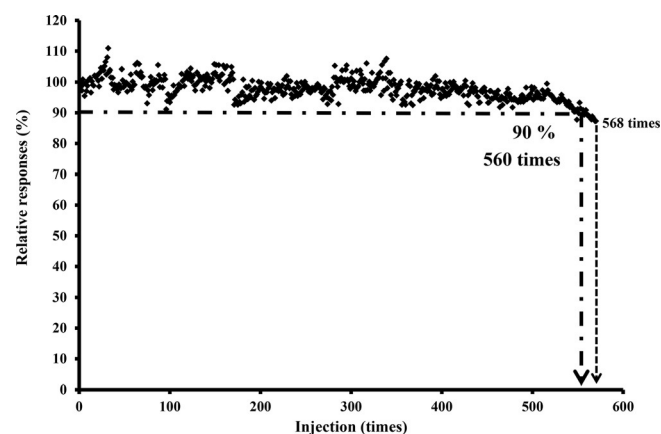
Fig. 6. The stability of electrode for the detection of 100 nM BPA in 100 mM phosphate buffer (pH 6.00) containing 0.10 M KCl, E = + 0.65 V versus Ag/AgCl.

sensitivity of the seven electrodes was also found to be only 2.5 % (Supporting Information Figure S5A inset). In addition, seven electrodes prepared on seven different days were also investigated. Almost the same results were found for all electrodes. The maximum RSD of the current responses was 3.2 % (Supporting Information Figure S5B) and the RSD of 2.4 % was obtained for the sensitivity of the seven electrodes (Supporting Information Figure S5B inset), reflecting a high repeatability for the fabrication of the porous gold electrodes.

3.7 Real Sample Analysis

The system was used to test for the leaching of BPA from polycarbonate bottles into water. The results from six brands of baby bottles at 40 °C and 100 °C showed that BPA was found in only one sample by both the amperometric and the GC-MS methods and with a higher value at a higher temperature (Supporting Information Table S2). Although BPA leaching was detected the amount was still lower than the safe value for the release of BPA, 50 μg L^{-1} (22 nM), set by the European Food Safety Authority (EFSA) [3]. The three brand of drinking water bottles were evaluated at room temperature and 40 °C. No BPA was detected from the drinking water bottles by either method (Supporting Information Table S3). The recoveries of BPA spiked into the samples were tested at 5.0, 10, 20 and 30 nM and were all found to be in the range of 89 %–103 % at 40 °C and 91 %–106 % at 100 °C for the baby bottles (Supporting Information Table S2), 94 %–102 % at room temperature and 89 %–103 % at 40 °C for the drinking water bottles (Supporting Information Table S3). This indicated the good accuracy of the methods (recommended recoveries; 70–120 % by AOAC at the analyte concentration levels of ppb and low ppm levels) [47]. Similar recoveries were obtained from the GC-MS, 93–105 % for baby bottles and 94–103 % for drinking water bottles (Supporting Information Table S2 and Table S3). The results indicated that the method developed for the determination of BPA that leaked from baby bottles and water bottles using the porous gold electrode was accurate and feasible.

4 Conclusions

A porous gold film was rapidly and simply fabricated directly onto a gold rod surface within 100 s by applying a potential step. Electrochemical observations showed that the unmodified porous gold electrode had a good electro-catalytic activity to oxidise the BPA. Compared to a bare gold surface it provided an improved oxidation peak current and a lower oxidation potential. A very low detection limit (2.0 ± 0.24 nM) was also obtained. The large surface area of the electrode illustrated its ability to minimize the fouling effect of the BPA oxidation products without any modification and/or cleaning step that could reduce the preparation and detection steps and increases the operation life of the electrode. The applicability for determining BPA in baby bottles and drinking water were successfully carried out by the proposed sensor with satisfactory recoveries (89–106 %) and the results were in good agreement with the GC-MS method (93–105 %). This porous gold electrode could be extremely useful for the determination of other organic substances, especially those with electrochemical products that formed an insulating layer on the electrode.

References

[1] L. N. Vandenberg, R. Hauser, M. Marcus, N. Olea, W. V. Welshons, *Reprod. Toxicol.* **2007**, *24*, 139–177.
[2] C. C. Willhite, G. L. Ball, C. J. McLellan, *J. Toxicol. Environ. Health, Pt. B Crit. Rev.* **2008**, *11*, 69–146.
[3] S. Biedermann-Brem, K. Grob, *Eur. Food Res. Technol.* **2008**, *228*, 679–684.
[4] G. D. Bittner, C. Z. Yang, M. A. Stoner, *Environ. Health* **2014**, *13*, 41–41.
[5] A. Karin, C. Paolo, H. Eddo, K. Spyridon, M. SHARON, P. Sazan, S. Dimosthenis, *Vol. 2015*, Publications Office of the European Union, **2010**.
[6] C. Simoneau, S. Valzacchi, V. Morkunas, L. Van den Eede, *Food Additives & Contaminants: Part A* **2011**, *28*, 1763–1768.
[7] H. Huang, Y. Li, J. Liu, J. Tong, X. Su, *Food Chem.* **2015**, *185*, 233–238.
[8] J. A. Rather, K. De Wael, *Sensors Actuators B: Chem.* **2013**, *176*, 110–117.
[9] M. Portaccio, D. Di Tuoro, F. Arduini, M. Lepore, D. G. Mita, N. Diano, L. Mita, D. Moscone, *Biosensors Bioelectron.* **2010**, *25*, 2003–2008.
[10] H.-s. Yin, Y.-l. Zhou, S.-y. Ai, *J. Electroanal. Chem.* **2009**, *626*, 80–88.
[11] F. Wang, J. Yang, K. Wu, *Anal. Chim. Acta* **2009**, *638*, 23–28.
[12] H. Yin, L. Cui, S. Ai, H. Fan, L. Zhu, *Electrochim. Acta* **2010**, *55*, 603–610.
[13] Y. Lin, K. Liu, C. Liu, L. Yin, Q. Kang, L. Li, B. Li, *Electrochim. Acta* **2014**, *133*, 492–500.
[14] S. Poorahong, C. Thammakhet, P. Thavarungkul, W. Limbut, A. Numnuam, P. Kanatharana, *Microchim Acta* **2012**, *176*, 91–99.
[15] E. Mazzotta, C. Malitesta, E. Margapoti, *Anal. Bioanal. Chem.* **2013**, *405*, 3587–3592.
[16] H. Zhang, J.-J. Xu, H.-Y. Chen, *The Journal of Physical Chemistry C* **2008**, *112*, 13886–13892.
[17] Y. Miao, L. Ouyang, S. Zhou, L. Xu, Z. Yang, M. Xiao, R. Ouyang, *Biosensors Bioelectron.* **2014**, *53*, 428–439.

[18] Z. Peng, H. Yang, *Nano Today* **2009**, *4*, 143–164.

[19] H. Yin, Y. Zhou, S. Ai, R. Han, T. Tang, L. Zhu, *Microchim Acta* **2010**, *170*, 99–105.

[20] J. Huang, X. Zhang, Q. Lin, X. He, X. Xing, H. Huai, W. Lian, H. Zhu, *Food Control* **2011**, *22*, 786–791.

[21] X. Tu, L. Yan, X. Luo, S. Luo, Q. Xie, *Electroanalysis* **2009**, *21*, 2491–2494.

[22] H.-J. Qiu, G.-P. Zhou, G.-L. Ji, Y. Zhang, X.-R. Huang, Y. Ding, *Colloids Surf. B. Biointerfaces* **2009**, *69*, 105–108.

[23] R. Li, D. Wu, H. Li, C. Xu, H. Wang, Y. Zhao, Y. Cai, Q. Wei, B. Du, *Anal. Biochem.* **2011**, *414*, 196–201.

[24] B. Y. Zhao, Q. Wei, C. Xu, H. Li, D. Wu, Y. Cai, K. Mao, Z. Cui, B. Du, *Sensors Actuators B: Chem.* **2011**, *155*, 618–625.

[25] Y. Deng, W. Huang, X. Chen, Z. Li, *Electrochem. Commun.* **2008**, *10*, 810–813.

[26] S. Trasatti, O. A. Petrii, *J. Electroanal. Chem.* **1992**, *327*, 353–376.

[27] a) S. Park, T. D. Chung, H. C. Kim, *Anal. Chem.* **2003**, *75*, 3046–3049; b) R. Szamocki, A. Velichko, C. Holzapfel, F. Mücklich, S. Ravaine, P. Garrigue, N. Sojic, R. Hempelmann, A. Kuhn, *Anal. Chem.* **2007**, *79*, 533–539.

[28] F. Jia, C. Yu, Z. Ai, L. Zhang, *Chem. Mater.* **2007**, *19*, 3648–3653.

[29] Q. Li, H. Li, G.-F. Du, Z.-H. Xu, *J. Hazard. Mater.* **2010**, *180*, 703–709.

[30] H. Kuramitz, M. Matsushita, S. Tanaka, *Water Res.* **2004**, *38*, 2331–2338.

[31] R. G. Compton, C. E. Banks, *Understanding Voltammetry*, 2nd ed., Imperial College Press, London, **2010**.

[32] H. Sambe, K. Hoshina, K. Hosoya, J. Haginaka, *J. Chromatogr.* **2006**, *1134*, 16–23.

[33] H. Yin, L. Cui, Q. Chen, W. Shi, S. Ai, L. Zhu, L. Lu, *Food Chem.* **2011**, *125*, 1097–1103.

[34] T. Łuczak, *Electrochim. Acta* **2008**, *53*, 5725–5731.

[35] Z. Liu, H. Zhang, S. Hou, H. Ma, *Microchim Acta* **2012**, *177*, 427–433.

[36] A. J. Bard, L. R. Faulkner, *Electrochemical Methods: Fundamentals and Applications*, 2nd ed., Wiley, New York **2000**.

[37] H. Yin, Y. Zhou, S. Ai, Q. Chen, X. Zhu, X. Liu, L. Zhu, *J. Hazard. Mater.* **2010**, *174*, 236–243.

[38] J. C. Hoogvliet, M. Dijksma, B. Kamp, W. P. van Bennekom, *Anal. Chem.* **2000**, *72*, 2016–2021.

[39] K.-J. Huang, Y.-J. Liu, Y.-M. Liu, L.-L. Wang, *J. Hazard. Mater.* **2014**, *276*, 207–215.

[40] X. Yan, C. Zhou, Y. Yan, Y. Zhu, *Electroanalysis* **2015**, *27*, 2718–2724.

[41] Y. Zhu, C. Zhou, X. Yan, Y. Yan, Q. Wang, *Anal. Chim. Acta* **2015**, *883*, 81–89.

[42] J. Yang, S.-E. Kim, M. Cho, I.-K. Yoo, W.-S. Choe, Y. Lee, *Biosensors Bioelectron.* **2014**, *61*, 38–44.

[43] a) C. Punckt, M. A. Pope, I. A. Aksay, *The Journal of Physical Chemistry C* **2013**, *117*, 16076–16086; b) J. Patel, L. Radhakrishnan, B. Zhao, B. Uppalapati, R. C. Daniels, K. R. Ward, M. M. Collinson, *Anal. Chem.* **2013**, *85*, 11610–11618; c) S. Saraf, C. J. Neal, S. Park, S. Das, S. Barkam, H. J. Cho, S. Seal, *RSC Advances* **2015**, *5*, 46501–46508.

[44] A. Özcan, *Electroanalysis* **2014**, *26*, 1631–1639.

[45] L. Peng, S. Dong, H. Xie, G. Gu, Z. He, J. Lu, T. Huang, *J. Electroanal. Chem.* **2014**, *726*, 15–20.

[46] C. Fang, N. M. Bandaru, A. V. Ellis, N. H. Voelcker, *J. Mater. Chem.* **2012**, *22*, 2952–2957.

[47] P. Bruce, P. Minkkinen, M.-L. Riekkola, *Mikrochim. Acta* **1998**, *128*, 92–106.